

# Siloxene, Germanane, and Methylgermanane: Functionalized 2D Materials of Group 14 for Electrochemical Applications

Nur Farhanah Rosli, Nasuha Rohaizad, Jiri Sturala, Adrian C. Fisher, Richard D. Webster, and Martin Pumera\*

2D monoelemental group 14 materials beyond graphene, such as silicene and germanene, have recently gained a lot of attention. Covalent functionalization of group 14 layered materials can lead to significant tuning of their properties. While optical and electronic properties of germanene, silicene, and their derivatives have been studied in detail previously, there is no information on their electrochemistry and toxicity. Herein, electrochemical applications of 2D siloxene, germanane, and methylgermanane, specifically for detection of an important biomarker, dopamine, as well as catalyzation of oxygen reduction and hydrogen evolution reactions, which are important in energy applications, are explored. Among the three materials, germanane portrays most superior properties for the electrochemical applications mentioned. All three materials possess fast heterogeneous electron transfer rates, relative to bare glassy carbon electrodes. In addition, toxicity studies of these materials are conducted to gain insights on their possible harmful effects toward human health. The results of this study show siloxene nontoxic while germanane and methylgermanane impose dose-dependent toxicity. Interestingly, methylation successfully reduce the toxicity of methylgermanane at lower concentrations. These studies provide fundamental insights into electrochemical and toxic properties of functionalized group 14 layered materials for future electrochemical applications.

## 1. Introduction

The groundbreaking research on graphene<sup>[1]</sup> has ignited intense interest in various 2D elemental nanomaterials.<sup>[2–9]</sup> These materials include group 14 mono-elemental graphene analogs known as silicene and germanene. Similar to graphene, they are 2D materials arranged in a honeycomb structure.<sup>[10]</sup> However, they have buckled sheets unlike graphene which is planar.<sup>[11,12]</sup> They exhibit similar promising electronic properties to graphene including low effective masses and high carrier mobilities but have a similarly negligible bandgap, which restricts their applications in electronics.<sup>[13]</sup> In addition, silicene and germanene are mainly synthesized on substrates due to lack of thermodynamic stability.<sup>[2,14]</sup> Hence, various modifications of silicene and germanene have been carried out to improve their stability and increase their bandgaps. Several modified silicene and germanene analogs were reported, e.g.,

N. F. Rosli, N. Rohaizad, Prof. R. D. Webster  
Division of Chemistry and Biological Chemistry  
School of Physical and Mathematical Sciences  
Nanyang Technological University  
21 Nanyang Link, Singapore 637371, Singapore

N. Rohaizad  
NTU Institute for Health Technologies  
Interdisciplinary Graduate School  
Nanyang Technological University  
61 Nanyang Drive, Singapore 637335, Singapore

Dr. J. Sturala  
Department of Inorganic Chemistry  
University of Chemistry and Technology Prague  
Technická 5, 166 28 Prague 6, Czech Republic

Prof. A. C. Fisher  
Department of Chemical Engineering and Biotechnology  
University of Cambridge  
New Museums Site  
Pembroke Street, Cambridge CB2 3RA, UK

 The ORCID identification number(s) for the author(s) of this article can be found under <https://doi.org/10.1002/adfm.201910186>.

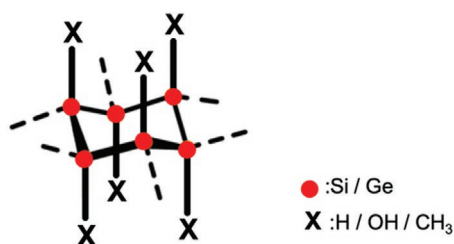
Prof. M. Pumera  
Center for Advanced Functional Nanorobots  
Department of Inorganic Chemistry  
University of Chemistry and Technology Prague  
Technická 5, 166 28 Prague 6, Czech Republic  
E-mail: martin.pumera@ceitec.vutbr.cz, pumera.research@gmail.com

Prof. M. Pumera  
Department of Chemical and Biomolecular Engineering  
Yonsei University  
50 Yonsei-ro, Seodaemun-gu, Seoul 03722, South Korea

Prof. M. Pumera  
Department of Medical Research  
China Medical University Hospital  
China Medical University  
No. 91 Hsueh-Shih Road, Taichung 40402, Taiwan

Prof. M. Pumera  
Future Energy and Innovation Laboratory  
Central European Institute of Technology  
Brno University of Technology  
Purkyňova 656/123, Brno CZ-616 00, Czech Republic

DOI: 10.1002/adfm.201910186



**Scheme 1.** Chemical structure of siloxene ( $\text{Si}_6\text{H}_3(\text{OH})_3$ ), germanane ( $\text{Ge}_6\text{H}_6$ ), and methylgermanane ( $\text{Ge}_6(\text{CH}_3)_6$ ).

siloxene ( $\text{Si}_6\text{H}_3(\text{OH})_3$ ), germanane ( $\text{Ge}_6\text{H}_6$ ), or methylgermanane ( $\text{Ge}_6(\text{CH}_3)_6$ ) (**Scheme 1**).

Siloxene, germanane, and methylgermanane can be prepared by topochemical deintercalation of their Zintl phases. Siloxene is  $-\text{H}$  and  $-\text{OH}$  modified silicene, prepared by topochemical deintercalation of Zintl phase  $\text{CaSi}_2$ .<sup>[15–18]</sup>  $\text{CaSi}_2$  possess interconnected  $\text{Si}_6$  rings in puckered arrangements held together by  $\text{Ca}^{2+}$  cations in a planar layered structure. These  $\text{Ca}^{2+}$  interlayers can be removed without disrupting the Si sheets, leaving each Si atom terminated by either  $-\text{H}$  or  $-\text{OH}$ . Siloxene is reported to be semiconducting and has a direct bandgap.<sup>[19]</sup> Meanwhile, germanane which is essentially hydrogen-terminated germanene is typically prepared by topochemical deintercalation of  $\text{CaGe}_2$ .<sup>[20]</sup> The hydrogenation termination of germanene results in the opening of bandgap which alters its electronic properties.<sup>[21]</sup> Germanane is semiconducting, possesses a direct bandgap with strong infrared photoluminescence.<sup>[22]</sup> Other unique properties of germanane include thermal stability and high resistance towards oxidation.<sup>[22]</sup> On the other hand, methyl-terminated germanene, methylgermanane, was first synthesized by Jiang et al.<sup>[23]</sup> and found to be semiconducting and have a direct bandgap of 1.76 eV.<sup>[24]</sup> Some interesting properties of methylgermanane includes strong photoluminescence, band edge fluorescence as well as improved thermal stability.<sup>[23]</sup> Methylgermanane is also reported with higher resistance against oxidation than germanane.<sup>[23]</sup>

Due to their unique and promising properties, these materials have been extensively explored for several applications. Siloxene has been reported as a promising photocatalyst for efficient water-splitting reactions,<sup>[19]</sup> an anode material in  $\text{Na}^+$ ,  $\text{Li}^+$ , and  $\text{K}^+$  ion batteries,<sup>[25]</sup> and a novel material for electrodes used for high-performance supercapacitor.<sup>[26]</sup> Germanane is reported to exhibit photocatalytic properties toward hydrogen generation through water splitting and hydrolysis of ammonia-borane complex.<sup>[27,28]</sup> Methylgermanane has been reported as a fluorescence marker on nanographene–platinum microrobots and photocatalysts for hydrogen generation.<sup>[27–30]</sup>

To the best of our knowledge, electrochemical applications of siloxene ( $\text{Si}_6\text{H}_3(\text{OH})_3$ ), germanane ( $\text{Ge}_6\text{H}_6$ ), and methylgermanane ( $\text{Ge}_6\text{Me}_6$ ) remain unexplored. In this study, we focus on investigating their electrochemical detection and catalization properties specifically for detection of an important biomarker, dopamine (DA), as well as the catalysis of important energy reactions, which includes the oxygen reduction and hydrogen evolution reactions (ORR and HER). In addition, we further examine their toxic properties to understand the safety risks they may pose to the human health. Prior to any electroanalysis studies, the materials were characterized to deeper comprehend their respective properties.

## 2. Results and Discussion

### 2.1. Characterization Studies

Scanning electron microscopy (SEM) in **Figure 1A–C** shows all materials with structural features typical of their bulk forms. Siloxene (**Figure 1A**) and methylgermanane (**Figure 1C**) appear to have sheet-like morphologies,<sup>[26,30]</sup> while germanane (**Figure 1B**) appears to have a layered block-like morphology with more angular edges.<sup>[27]</sup> Elemental maps obtained from energy dispersive spectroscopy (EDS) show homogeneous distribution of Si and O for siloxene (**Figure S1A**, Supporting Information), Ge for germanane (**Figure S1B**, Supporting Information), and Ge and C for methylgermanane (**Figure S1C**, Supporting Information). Oxygen is observed on germanane and methylgermanane indicating small degree of material oxidation whereas carbon is observed only on germanane attributing to carbon from carbon tape and adventitious carbon from the environment. In addition, atomic force microscopy (AFM) was conducted to study the thickness and size of the materials (**Figure S2**, Supporting Information). The results obtained show that siloxene have width ranging between 2 and 3  $\mu\text{m}$  while its thickness varies from about 100 to 800 nm. Similarly, methylgermanane possess width ranging from 2 to 3.5  $\mu\text{m}$  but with thickness of only 100 to 300 nm. Germanane has the largest size as its width was measured as 4  $\mu\text{m}$  and with thickness of about 200 nm.

The materials were then characterized by X-ray powder diffraction (XRD) and high-resolution transmission electron microscopy (HR-TEM). From the XRD analyses (**Figure 2**), the diffuse peaks suggest that the materials are more amorphous than crystalline, which is in accordance with 2D nature of these materials. From the XRD, the interlayer distance between two methylgermanane (GeMe) sheets is 8.9 Å ( $2\theta 10.0^\circ$ ). Germanane (GeH), which contains less bulky hydrogen instead of methyl

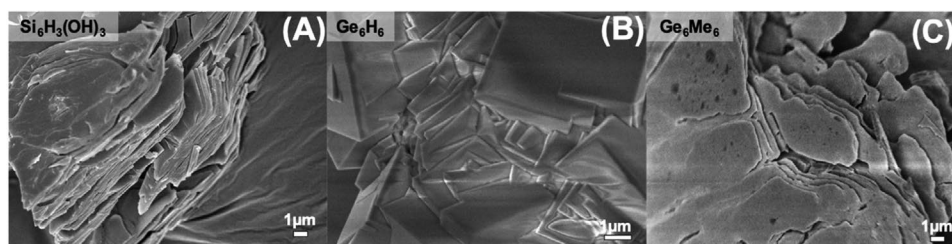


**Figure 1.** SEM images of A) siloxene, B) germanane, and C) methylgermanane.

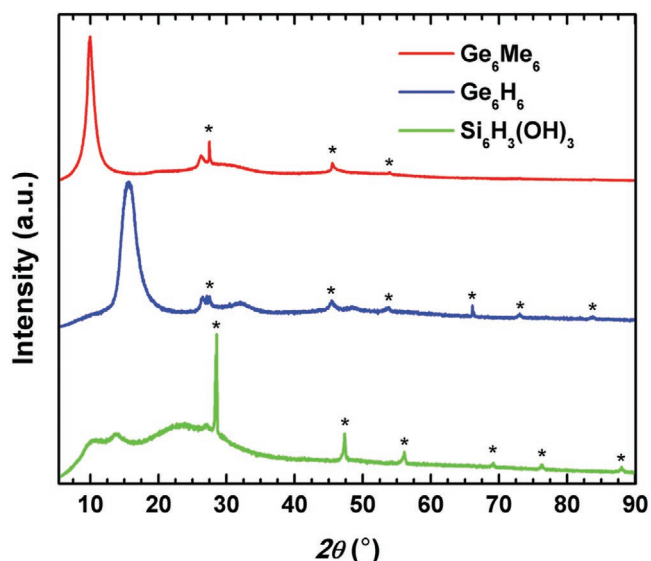


**Figure 2.** XRD spectra of methylgermanane, germanane, and siloxene. Star labeled peaks correspond to residual germanium or silicon, respectively.

groups, has interlayer distance 5.7 Å ( $2\theta$  15.6°). For siloxene, the interlayer distance is about 6.4 Å ( $2\theta$  13.8°). These amorphous structures were also confirmed by HR-TEM (Figure S3, Supporting Information). All materials contain traces of residual germanium or silicon (labeled by star in Figure 2), respectively.

Next, X-ray photoelectron spectroscopy (XPS) was employed to further confirm the elemental compositions of the materials. The XPS survey scans in Figure S4A–C (Supporting Information) show Si, Ge, C, and O peaks as anticipated. C and O peaks are seen due to surface functionalization, oxidation of materials or exposure to adventitious C and O. In addition, Cl peaks are found in siloxene and germanane while an iodine peak is observed in methylgermanane as methyl iodide was involved in the preparation of materials. These impurities have been previously reported in other studies.<sup>[20,23]</sup> High-resolution XPS (HR-XPS) was conducted to deeper analyze the success of modification and the corresponding chemical environments of the materials. The modification of silicene to siloxene leads to the formation of –H and –OH bonds on Si.<sup>[16]</sup> These bonds can be confirmed from HR-XPS Si 2p and O 1s scans. The Si 2p scan (Figure 3A) shows two peaks centered at 102.4 and 99.8 eV,

which are attributed to Si–O and Si–H peaks, respectively.<sup>[19,26,31]</sup> An O 1s scan of siloxene (Figure S4D, Supporting Information) shows two peaks centered at 531 and 529.8 eV attributed to Si–O and adventitious oxygen (e.g., intercalated water) peaks, respectively.<sup>[26,31]</sup> Adventitious oxygen is present due to exposure of samples to the atmosphere. The modification of calcium germanide to germanane and methylgermanane resulted in the formation of Ge–H and Ge–C bonds respectively. From HR-XPS Ge 3d scans of germanane (Figure 3B) and methylgermanane (Figure 3C), peaks centered at 29.8 and 31.1 eV are observed and attributed to Ge–H and Ge–C, respectively.<sup>[27,28]</sup> The successful formation of –H and –C bonds on Ge are confirmed by peak shifts to higher binding energies relative to elemental Ge.<sup>[32]</sup> Ge–C resulted in a larger shift in binding energy as compared to Ge–H as electronegativity of C is higher than H.<sup>[33,34]</sup> In addition, C 1s peak belonging to Ge–C was observed at 282.3 eV confirming the bonding of C on Ge.<sup>[30]</sup> Other peaks obtained from HR-XPS of O 1s and C 1s (Figure S4E–I, Supporting Information) are attributed to adventitious C and O due to the exposure of materials to the atmosphere.

The materials were then characterized by Fourier transformed infrared (FTIR) spectroscopy. The FTIR spectrum of siloxene (Figure S5A, Supporting Information) shows distinct peaks corresponding to Si–OH and Si–H at 1008 and 2104  $\text{cm}^{-1}$ .<sup>[25,26,31,35]</sup> FTIR spectra of germanane (Figure S5C, Supporting Information) and methylgermanane (Figure S5E, Supporting Information) both show absorption bands corresponding to H<sub>2</sub>O (1635  $\text{cm}^{-1}$ ). In addition, methylgermanane possess absorption bands for Ge–C (530  $\text{cm}^{-1}$ ) and CH<sub>3</sub> at 769, 1236, and 2906  $\text{cm}^{-1}$  while germanane have Ge–H bands at 472 and 1998  $\text{cm}^{-1}$ .<sup>[20,22,23,36]</sup> Following that, the crystallinity and bonding nature of the materials were studied by Raman spectroscopy. Figure S5B (Supporting Information) shows the Raman spectrum of siloxene with one main band at 497  $\text{cm}^{-1}$  corresponding to Si–O vibrations. Several weaker bands are also observed at 380  $\text{cm}^{-1}$  consistent with Si–Si vibrations as well as 636, 732, and 2119  $\text{cm}^{-1}$  attributed to Si–H vibrations.<sup>[19–26,31]</sup> Raman spectra of germanane (Figure S5D, Supporting Information) and methylgermanane (Figure S5F, Supporting Information) have observable peaks at  $\approx 300$   $\text{cm}^{-1}$  consistent with the Ge–Ge vibration  $E_2$  mode.<sup>[22,36]</sup> These characterization results are in close agreement to our previous work which implies successful synthesis of materials.<sup>[37]</sup>

As the experiments were performed in the aqueous conditions, stability of these materials could be an issue. Therefore,

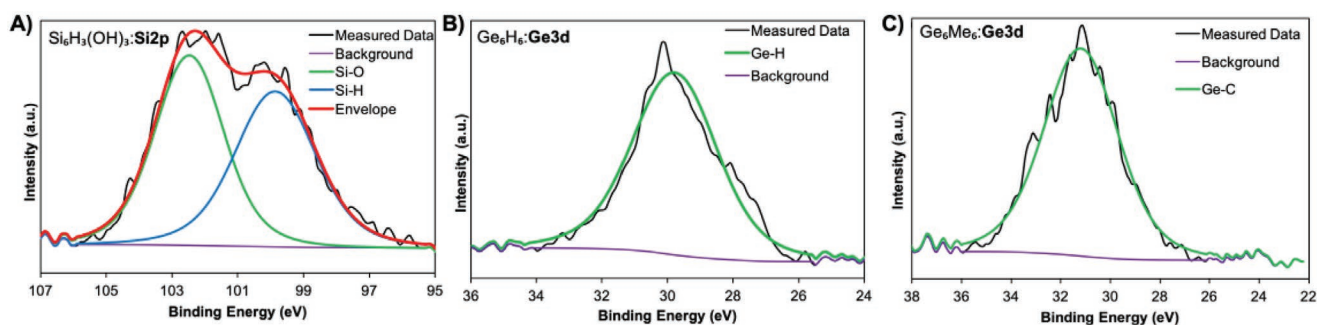


**Figure 3.** HR-XPS scans of A) Si 2p from siloxene, B) Ge 3d from germanane, and C) Ge 3d from methylgermanane.

stability test of these materials were performed by measuring FTIR and Raman spectra before and after 1 week in water. According to the spectra, there is no obvious change in material composition (Figures S6 and S7, Supporting Information). FTIR spectra were measured on diamond ATR, therefore, the scale between 1950 and 2200  $\text{cm}^{-1}$  is not displayed.

## 2.2. Fundamental Electrochemical Studies

Understanding fundamental electrochemical properties of materials is important for their prospective applications. Inherent electrochemical properties of siloxene, germanane, and methylgermanane were explored to understand their intrinsic redox behavior upon application of an electrochemical potential. To study this, glassy carbon (GC) electrodes were modified by these materials respectively and cyclic voltammetry was performed over a potential range of  $-1.5$  to  $+1.5$  V in phosphate buffered saline (PBS) electrolyte as presented in Figure 4A. From the results, an irreversible oxidation peak is observed at  $+0.7$  V for methylgermanane while the others have negligible redox peaks. This implies that oxidation of  $\text{Ge}^+$  to higher oxidation states, possibly  $\text{Ge}^{2+/3+}$ , have occurred. One possible reason is that a few Ge atoms are still exposed

on the surface of the material as the bulky methyl groups are not fully covering the Ge layers, resulting in the occurrence of oxidation.<sup>[38]</sup> Since inherent properties may limit the operating potential window of materials, the absence of peaks in siloxene and germanane allows more opportunities for prospective electrochemical applications.<sup>[39,40]</sup>

Next, we set forth to study the rate of heterogeneous electron transfer (HET), an important factor for assessing the compatibility of material for electrochemical applications. A fast HET rate suggests fast kinetics and is therefore a desirable attribute of a prospective electrode material. To study HET, cyclic voltammetry of  $[\text{Fe}(\text{CN})_6]^{3-/4-}$  redox probe in KCl (0.1 M) with material modified electrodes were studied. The results in Figure 4B show shifts in cathodic and anodic peaks, which brought about a change in peak-to-peak separation ( $\Delta E_p$ ). The  $\Delta E_p$  values are presented in Figure 4C. Germanane and methylgermanane have lower  $\Delta E_p$  values of 155 and 138 mV, respectively, while siloxene has a higher  $\Delta E_p$  of 248 mV which suggest HET rates for germanium materials are relatively higher. Nevertheless, all three materials possess smaller  $\Delta E_p$  than GC which implies that modification of electrode with these materials can successfully improve HET rates. To confirm this, HET rate constants ( $k_{\text{obs}}^0$ ) were then obtained from  $\Delta E_p$  values which are presented in Table S1 (Supporting Information). The

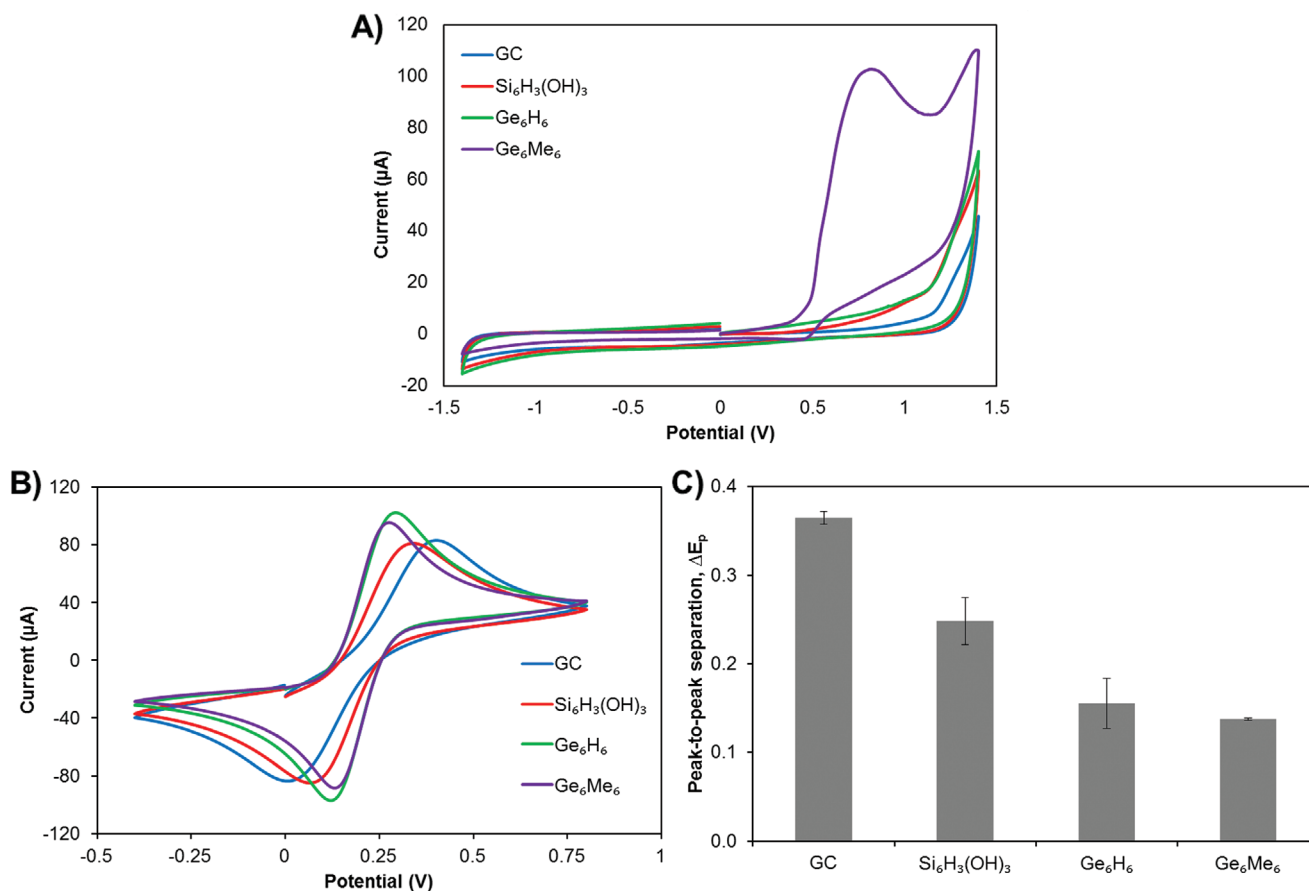


**Figure 4.** Cyclic voltammograms (CVs) of GC, siloxene, germanane, and methylgermanane in A) PBS ( $50 \times 10^{-3}$  M), B)  $[\text{Fe}(\text{CN})_6]^{3-/4-}$  redox probe ( $10 \times 10^{-3}$  M) in KCl (0.1 M), and C) peak-to-peak separations ( $\Delta E_p$ ) with their corresponding standard deviation. All measurements are performed using Pt counter electrode at a scan rate  $100 \text{ mV s}^{-1}$  versus Ag/AgCl reference electrode.

calculated  $k_{\text{obs}}^0$  of siloxene is 5 times higher than that of GC, while the calculated  $k_{\text{obs}}^0$  of germanane and methylgermanane,  $2.01 \times 10^{-3}$  and  $2.57 \times 10^{-3} \text{ cm s}^{-1}$  respectively, are  $\approx 17$  and 21 times higher than the  $k_{\text{obs}}^0$  of GC ( $1.18 \times 10^{-4} \text{ cm s}^{-1}$ ). In a nutshell, germanane and methylgermanane have high HET rates (compared to GC), which is a favorable property for electrode materials in electrochemical applications.

### 2.3. Electrochemical Detection

Generally, due to high HET rates, 2D materials can be integrated on electrode surfaces to increase selectivity and sensitivity of electrochemical sensors to target molecules.<sup>[41,42]</sup> Properties such as large surface area, enhanced mass transport, excellent signal-to-noise ratios, and high sensitivity have resulted in the vast incorporation of 2D materials in sensing applications.<sup>[43]</sup> DA is a vital neurotransmitter in the brain for optimal performance of the central nervous system, cardiovascular system, and hormonal system. DA in abnormal levels has been known to lead to conditions such as Parkinson's disease, schizophrenia, attention deficit hyperactivity disorder, and restless legs syndrome (RLS).<sup>[44]</sup> However, detection of DA is challenging owing to its low physiological concentration along with interferences from other biomolecules, specifically

ascorbic acid (AA) and uric acid (UA), due to overlapping oxidation potentials.<sup>[45,46]</sup> Since then, novel 2D materials have been explored to enhance selectivity and sensitivity of DA detection.<sup>[45–51]</sup> Commonly reported materials are carbon-based and gold-based materials.

As DA is an electroactive species, cyclic voltammetry (CV) and differential pulse voltammetry (DPV) were performed to evaluate the performance of siloxene, germanane, and methylgermanane modified electrodes for selective detection of dopamine. The redox reaction of dopamine involves two electrons transfer to form dopamine *o*-quinone and this two electrons transfer can be detected electrochemically.<sup>[52]</sup> Since DA commonly coexists with AA and UA in biological samples, a selective detection is highly desired. CV was performed with the modified electrodes in a solution mixture containing AA ( $1.0 \times 10^{-3} \text{ M}$ ), UA ( $0.1 \times 10^{-3} \text{ M}$ ), and DA ( $0.1 \times 10^{-3} \text{ M}$ ). These respective concentrations are chosen as the commonly reported linear range of AA is generally higher than that of UA and DA.<sup>[46]</sup> From **Figure 5A**, two distinct peaks are seen from the germanane modified electrode (green line) at +0.42 and +0.61 V. Similarly, the methylgermanane modified electrode (purple line) show distinct separation of peaks at +0.38 and +0.65 V. However, peak currents from methylgermanane are significantly lower than that of germanane. This suggests that methylgermanane possesses selectivity but lacks sensitivity. Bare GC (blue line) and siloxene modified electrode (red line) both have negligible peak separations which eliminates siloxene as a material for selective detection of DA.

After establishing germanane as the most promising material with high selectivity and sensitivity, the identities of the peaks were investigated. In **Figure 5B**, germanane was utilized to detect AA, UA, and DA simultaneously and individually as a comparison. The peak potentials of AA and UA are observed to be close to each other specifically, at +0.31 V (red line) and +0.40 V (blue line) respectively. As the peaks are close together, simultaneous detection of the UA and AA results in an overall broad peak centered at +0.42 V as seen in the simultaneous scan (black line). However, the peak potential of DA is found at a higher potential of +0.64 V (green line) and is reflected as a separate peak in the simultaneous scan (black line). This shows that the germanane modified electrode can separately detect DA from AA and UA due to its higher peak potential. Hence, germanane can aid in the selective detection of DA with good sensitivity.

Following that, DPV was used for calibration studies of DA. In **Figure S8A** (Supporting Information), an increase in peak currents with increasing concentration of DA is observed. The respective current peaks are obtained and plotted against the concentration of DA (**Figure S8B**, Supporting Information). In the range of  $30 \times 10^{-6}$  to  $100 \times 10^{-6} \text{ M}$  of dopamine, a linear relationship was obtained with a correlation coefficient of  $R^2 = 0.988$ . The limit of detection (LOD) and limit of quantification (LOQ) values were found to be  $19.1 \times 10^{-6}$  and  $63.9 \times 10^{-6} \text{ M}$  respectively. To calculate sensitivity, the electroactive surface area is foremostly required. CVs were performed for the germanane modified electrodes in ferro/ferri at different scan rates (**Figure S9A**, Supporting Information). The measured anodic current is plotted against square root of scan rate, showcasing a linear relationship which implies a diffusion controlled process

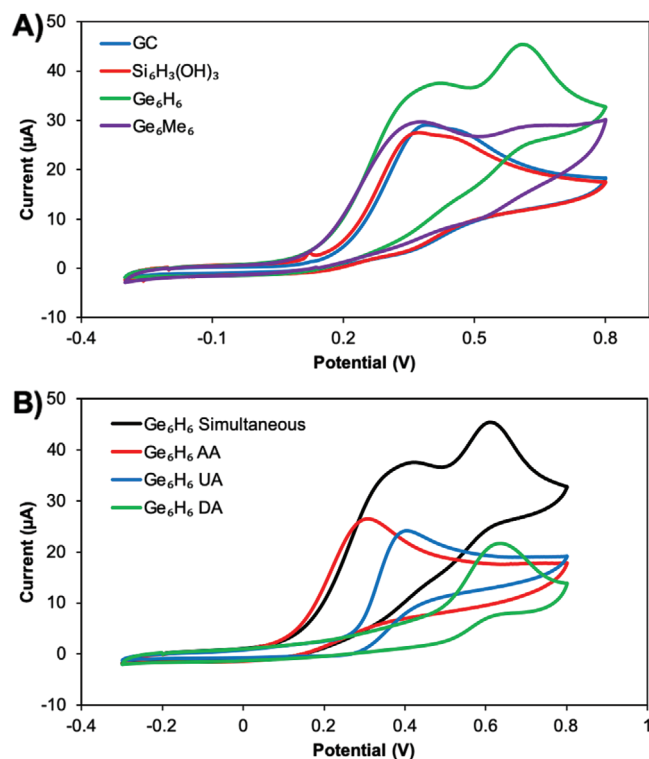


**Figure 5.** A) Cyclic voltammograms (CVs) obtained with GC, siloxene, germanane, and methylgermanane modified electrodes with simultaneous addition of AA ( $1.0 \times 10^{-3} \text{ M}$ ), UA ( $0.1 \times 10^{-3} \text{ M}$ ), and DA ( $0.1 \times 10^{-3} \text{ M}$ ). B) CVs obtained with germanane modified electrode with simultaneous addition of AA, UA, and DA (black line); AA only (red line); UA only (blue line); and DA only (green line). These measurements were performed in PBS ( $50 \times 10^{-3} \text{ M}$ ) using Pt counter electrode at a scan rate of  $100 \text{ mV s}^{-1}$  versus Ag/AgCl reference electrode.

(Figure S9B, Supporting Information). At the same time, the gradient obtained from Randles-Sevcik equation,

$$i_p = 0.446nFAC^0 \left( \frac{nFvD_0}{RT} \right)^{1/2} \quad (1)$$

was used to compute the electroactive surface area,  $A$ . Sensitivity is then obtained to be  $0.308 \mu\text{A } \mu\text{M}^{-1} \text{cm}^{-2}$ . Stability of germanane modified electrodes after 1, 3, and 6 days were investigated by monitoring the changes to DA peak obtained from DPV (Figure S10A, Supporting Information). The peak potentials were found to be unaltered but a slight decrease in peak currents were observed. As compared to the initial current measured on day 1, peak currents on day 3 and day 6 decreased to 94% and 90%, respectively (Figure S10B, Supporting Information). These decrease are near negligible which show that germanane modification on GC electrodes have relatively high stability. Additionally, the effect of pH on the detection properties of DA was investigated. Figure S11 (Supporting Information) present voltammograms of germanane-modified electrodes in the presence of DA, UA, and AA at varying pH of 2, 4, 6, 7, 8, and 10. From the results obtained, pH 6, 7, and 8 have distinct separations of DA peaks from UA and AA, allowing selective detection of DA. These peaks were found at the same potential of +0.64 V. However, peak current in pH 7 is found to be twice as high as that in pH 6 and 8. There are no observable peak separations in pH 2, 4, and 10. This shows that a neutral pH is optimum for detection of DA whereas acidic and alkaline pH diminish the selectivity of DA detection.

Previously, 2D siloxene sheets have been reported as a novel electrochemical sensor for selective dopamine detection. Ramachandran et al.<sup>[53]</sup> showed that these 2D siloxene sheets possessed great improvements in performance as compared to the materials studied herein. This is due to their thin sheet-like nature which directly suggest that size greatly influence the performance of siloxene as material for sensor. Hence, reducing the size and thickness of germanane and methylgermanane could also possibly improve their performance tremendously.

## 2.4. Electrocatalytic Performance

In this section, we report on the electrocatalytic performances of siloxene, germanane, and methylgermanane in energy applications, specifically for the ORR and HER. ORR is an essential cathode reaction in fuel cells for energy production while HER is the cathodic half reaction for water splitting in fuel production.<sup>[54,55]</sup> These are important reactions in energy applications and several studies aiming at improve their costs and efficiency have been conducted. To date, noble metals such as platinum (Pt) remain to be the best performing catalyst with highest efficiency but are not economically favorable.<sup>[56]</sup> As such, the search for cheaper alternatives with similar catalytic efficiency is growing.

Electrocatalytic performance toward ORR was investigated by linear sweep voltammetry (LSV) in KOH (0.1 M). Their performances are compared with the catalytic performance of Pt, more commonly used in the form of Pt/C.<sup>[55]</sup> In ambient conditions (solid lines), the cathodic current decreases due

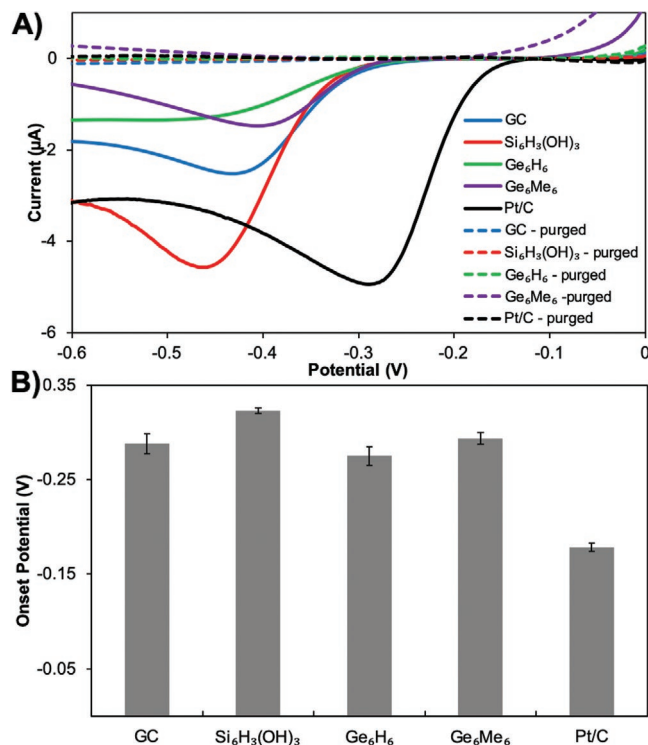


**Figure 6.** A) Linear sweep voltammograms for ORR in ambient (solid line) and N<sub>2</sub>-purged (dotted line) conditions. B) Average onset potentials with respective standard deviations of GC, siloxene, germanane, methylgermanane, and Pt/C. All measurements were performed in KOH (0.1 M) using Pt counter electrode at a scan rate of 5 mV s<sup>-1</sup> versus Ag/AgCl reference electrode.

to a direct 4-electron reduction pathway from O<sub>2</sub> to H<sub>2</sub>O in aqueous solution.<sup>[57]</sup> From **Figure 6A**, the respective reduction peaks attributed to ORR were clearly observed. The identities of these ORR peaks were verified by conducting the experiments in N<sub>2</sub>-purged conditions (dotted lines) in which the peaks are absent in oxygen-free conditions. The electrocatalytic ORR performances of the materials were analyzed using onset potentials; the potential at which 10% of the maximum current is reached, as presented in **Figure 6B**. Overall, the onset potentials of siloxene, germanane, and methylgermanane are higher than Pt/C indicating weaker ORR catalytic performance. Nonetheless, germanane possesses a slightly lower onset potential than bare GC, -0.28 and -0.29 V respectively, but siloxene and methylgermanane have slightly higher onset potentials than bare GC specifically, -0.32 and -0.29 V respectively, indicating unfavorable electrocatalytic performance for ORR.

Next, electrocatalytic performance toward the HER was investigated by LSV in H<sub>2</sub>SO<sub>4</sub> (0.5 M) (**Figure 7A**) and analyzed by comparing their respective overpotential; that is, the potential at which the current density of -10 mA cm<sup>-2</sup> is achieved. Overpotential is commonly used as a performance indicator of the HER efficiency in energy applications, with lower overpotentials indicating higher catalytic performance for the HER.<sup>[58]</sup> It is clear that Pt/C has the lowest overpotential of -0.14 V indicating superior electrocatalytic performance toward the HER as compared to others. Siloxene and methylgermanane have higher overpotentials than GC indicating poorer electrocatalytic

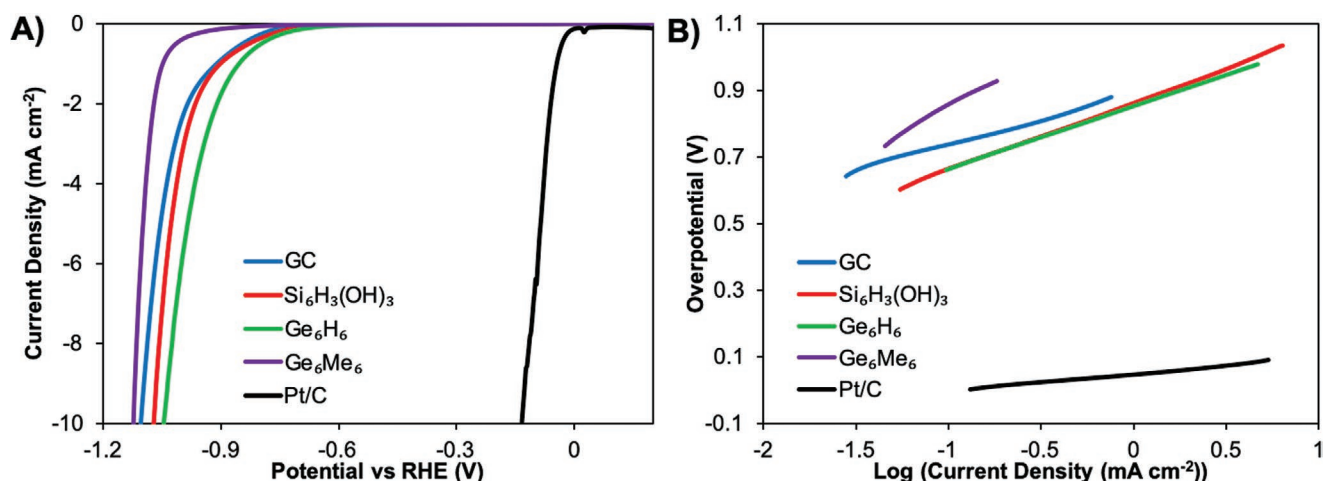
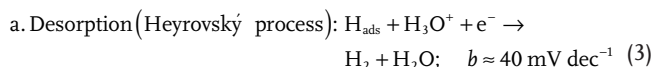
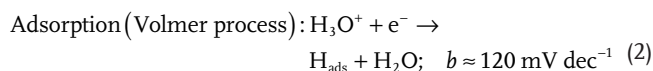


**Figure 7.** A) Linear sweep voltammograms for HER and B) Tafel plots of GC, siloxene, germanane, methylgermanane, and Pt/C with respective standard deviations. All measurements are performed in H<sub>2</sub>SO<sub>4</sub> (0.5 M) using bare GC counter electrode at a scan rate of 2 mV s<sup>-1</sup> versus RHE.

performance for the HER but germanane has a lower overpotential than bare GC, -1.04 and -1.11 V respectively, suggesting improved electrocatalytic performance for the HER. Similar to the ORR, only germanane showed improvement as the catalyst for the HER in comparison to bare GC. Apart from the HER overpotential, Tafel slopes also evaluate the electrocatalytic ability for the HER and is employed to deduce the rate limiting step of a material. Tafel slopes,  $b$ , are obtained by plotting the linear range fitted to the Tafel equation of  $\eta = a + b \log |j|$ , where  $\eta$  is the overpotential and  $j$  is the current density as shown in Figure 7B. Following are possible rate limiting steps of the HER<sup>[59,60]</sup>



The first step of the HER is the formation of hydrogen atoms by adsorption followed by either a Heyrovský or Tafel desorption step. Out of the three materials, germanane produces the lowest Tafel slope value of 184 mV dec<sup>-1</sup> while the Tafel slope of siloxene and methylgermanane are higher, specifically 202 and 303 mV dec<sup>-1</sup>, respectively. Tafel slopes of all three materials suggest the rate limiting step to be a Volmer adsorption process, similar to that of bare GC (150 mV dec<sup>-1</sup>). Germanane has the best performance as an electrocatalyst for the HER among the three materials.

When comparing with other mono-elemental materials, siloxene, germanane, and methylgermanane have better HER performances than bulk pnictogens but weaker than shear exfoliation pnictogen nanosheets.<sup>[61]</sup> For ORR, these functionalized group 14 materials possess comparable performance to triple-layered and double-layered graphene but are weaker than few-layered 3D graphene and graphene with low oxygen content.<sup>[62,63]</sup> However, it should be mentioned that ORR on

graphene is often driven by residual Mn-based impurities.<sup>[64]</sup> Other 2D materials commonly reported as HER and ORR catalysts include transition metal dichalcogenides (TMDs) and transition metal oxides. Generally, HER catalytic performance of group 6 (Mo and Ws) TMDs<sup>[65]</sup> were reported to be higher whereas HER performance of group 4 (Ti, Zr, and Hf)<sup>[66]</sup> and group 5 (V, Nb, and Ta) TMDs were found comparable with an exception of VTe<sub>2</sub> which exhibited a much lower HER overpotential of 0.5 V.<sup>[67]</sup> The ORR catalytic performance of siloxene, germanane, and methylgermanane were found comparable with group 6 TMDs and transition metal oxides with an exception from Mn oxides which possessed low onset potentials indicating higher ORR catalytic performance.<sup>[64,68]</sup>

## 2.5. Toxicity Studies

Next, toxicity of siloxene, germanane, and methylgermanane were evaluated on four cell lines obtained from different parts of a human body, namely breast carcinoma (MCF-7), lung carcinoma (A549), kidney (HEK 293), and liver carcinoma (HepG2) cells. Toxicity is an important property to study prior to large scale usage of new materials<sup>[69,70]</sup> and toxicity of these materials have yet to be determined. This serves as a preliminary step toward investigating their biocompatibility for biological applications. Herein, cytotoxicity was assessed by evaluating cell viabilities after exposure to the respective materials in increasing concentrations. Cell viability was measured using cell counting kit-8 (CCK-8); a sensitive colorimetric cell proliferation assay whereby cell viability can be quantified by absorbance spectroscopy.<sup>[71]</sup>

The results obtained show varying toxic properties for different materials in different cell lines (Figure 8). Cells exposed to siloxene show no change in cell viability (red bars), which indicate negligible toxicity toward all cell lines. This is expected as several silicon-based materials are similarly reported to be nontoxic.<sup>[72-74]</sup> On the other hand, germanane and methylgermanane are found to induce dose-dependent toxicity on cells. Previously, studies have indeed reported high toxicity of

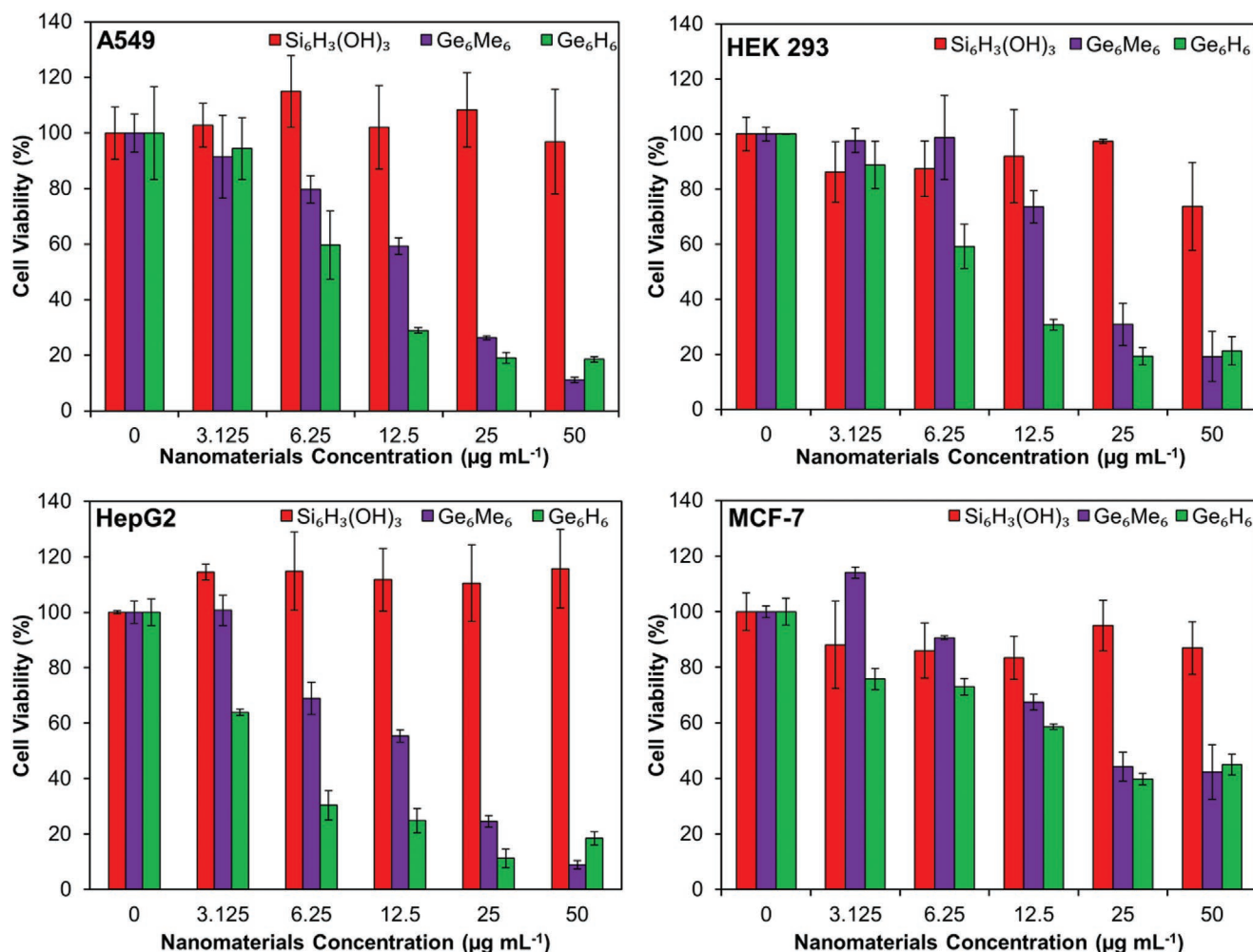


**Figure 8.** Percentage of cell viability for A549 cells, HEK 293 cells, HepG2 cells, and MCF-7 cells upon introduction of 0–50  $\mu\text{g mL}^{-1}$  of siloxene, germanane, and methylgermanane for 24 h with the respective standard deviations. Cell viability percentages were obtained from normalization of absorbance readings with readings of negative control.

germanium nanoparticles.<sup>[75]</sup> Additionally, our studies found germanane to be more toxic than methylgermanane, specifically in low concentrations (6.25 and 12.5  $\mu\text{g mL}^{-1}$ ). This implies that methylation of germanane can reduce toxicity in the lower concentration range. Notably, germanane and methylgermanane were both found to be most toxic toward HepG2 cells and least toxic toward MCF-7 cells. As an illustration, upon exposure of 3.125  $\mu\text{g mL}^{-1}$  of germanane, the cell viability reduced to 64% for HepG2 cells while the other cell lines remained above 75%. Likewise, upon exposure of 6.25  $\mu\text{g mL}^{-1}$  of methylgermanane to HepG2 cells, the cell viability reduced to 69% while other cells remained above 80%. The lowest viability of MCF-7 cells remained at 40% despite exposure of the highest concentration (50  $\mu\text{g mL}^{-1}$ ) of both materials. This implies that germanane and methylgermanane are more toxic toward liver cells and are more compatible toward breast cells.

Control studies of the respective materials were performed to eliminate assay interference which may lead to false results.<sup>[76,77]</sup> They were carried out with materials in the absence of cells to observe false positive and negative results due to interferences from the materials toward the assay

reagents. From the control studies, false positive results for germanane and methylgermanane were found. Due to this, a background removal step was implemented before analysis of cytotoxicity data above to obtain more accurate results. To elaborate, Figure S12A (Supporting Information) shows normalized absorbance measurements taken at 450 nm wavelength at different concentrations of materials. From the results, germanane and methylgermanane increased in absorbance with increasing concentration of materials which suggest possible interference. This was confirmed by obtaining absorbance spectra (350–550 nm) of respective materials in different concentrations in both the absence and presence of cells. For siloxene, absence of peaks was observed for the control set while peaks were observed in the presence of cells as expected (Figure S12B, Supporting Information). This is not the case for methylgermanane (Figure S12C, Supporting Information) and germanane (Figure S12D, Supporting Information) as peaks were observed in the spectra during both the absence and presence of cells. This implies that germanane and methylgermanane possess absorbance at these similar wavelengths which resulted in false

positive results. This may be due to strong light absorbance in the whole visible light region by germanane and methylgermanane as reported by Liu et al.<sup>[28]</sup>

### 3. Conclusion

Siloxene ( $\text{Si}_6\text{H}_3(\text{OH})_3$ ), germanane ( $\text{Ge}_6\text{H}_6$ ), and methylgermanane ( $\text{Ge}_6(\text{CH}_3)_6$ ) were successfully synthesized and functionalized as confirmed by characterization studies through SEM, AFM, HR-TEM, EDS, XPS, XRD, FTIR, and Raman spectroscopy. Following that, electrochemical properties studies show that they possessed relatively fast HET rates, compared to a bare GC electrode, which implies improved performance for electrochemical detection. Germanene-based materials were found to be superior to siloxene as they demonstrate faster HET rates and higher sensitivity for detection of DA. Between the two germanene-based materials, germanane portrayed the most sensitive detection of DA. Similarly, electrocatalytic studies found germanane to have the best electrocatalytic properties toward the ORR and HER with improved performance to a bare GC electrode. Toxicity studies show negligible toxic properties for siloxene but dose-dependent toxicity for germanane and methylgermanane. Interestingly, it is found that methylation can successfully reduce toxicity of germanene-based materials in a lower concentration range. Overall, germanane-based materials have more superior properties than siloxene, with germanane ( $\text{Ge}_6\text{H}_6$ ) as the best material for electrochemical applications. These studies provide essential fundamental insights into the electrochemical properties and toxicity of these functionalized group 14 layered materials for future electrochemical applications.

### 4. Experimental Section

**Synthesis of Materials:** Siloxene<sup>[78]</sup> ( $\text{Si}_6\text{H}_3(\text{OH})_3$ ):  $\text{CaSi}_2$  (0.500 g, 5.20 mmol) was treated with 35% aqueous hydrochloric acid (50 mL) at room temperature and stirred for 24 h. A yellowish solid was then collected by filtration and rinsed with 35% aqueous hydrochloric acid ( $2 \times 25$  mL), water ( $5 \times 100$  mL), and acetone ( $2 \times 50$  mL).

Germanane<sup>[22]</sup> ( $\text{Ge}_6\text{H}_6$ ):  $\text{CaGe}_2$  (1.000 g, 5.40 mmol) was added to 35% aqueous hydrochloric acid (100 mL) at  $-35$  °C and stirred for 7 d. A gray solid was then collected by filtration, washed with cold 35% aqueous hydrochloric acid ( $2 \times 25$  mL), water ( $5 \times 100$  mL), and acetone ( $2 \times 50$  mL).

Methylgermanane<sup>[23]</sup> ( $\text{Ge}_6\text{Me}_6$ ):  $\text{CaGe}_2$  (0.400 g, 2.16 mmol) and methyl iodide (5 mL, 11.4 g, 80.32 mmol) were inserted into a sintered glass funnel (pore size S4) and closed with parafilm. The bottom part of the funnel was filled with water and stirred for 7 d. The solid was collected by filtration, washed with water ( $5 \times 100$  mL), and acetone ( $3 \times 50$  mL).

The products were dried in vacuo and stored in the dark under an inert argon atmosphere.

**Instruments:** SEM and EDS were imaged by JEOL 7600F (Japan). Phoibos 100 spectrometer with a monochromatic Mg X-ray radiation source (SPECS, Germany) was used to obtain XPS data and analysis was carried out with CasaXPS software. InVia Raman microscope (Renishaw, England) in backscattering geometry with CCD detector, DPSS laser (532 nm, 50 mW) with applied power of 10 mW was used for Raman spectroscopy measurements. FTIR measurements

were performed on an iS50R FTIR spectrometer (Thermo Scientific, USA).  $\mu$ Autolab type III electrochemical analyzer (Eco Chemie, The Netherlands) was used to conduct electrochemical measurements and analysis was carried out using NOVA version 1.10 software. Thermo Multiskan GO was used to measure absorbance readings and analyses were carried out by Skanlt software for microplate readers (Thermo Fisher Scientific, Singapore).

**Electrochemical Measurements:** The materials were dispersed in ultrapure water ( $2.5 \text{ mg mL}^{-1}$ ) and subjected to 1 h of ultrasonication to obtain well-dispersed suspensions. Prior to electrochemical measurements, the suspensions were subjected to an addition of 10 min of ultrasonication to maintain well-dispersed samples. For electrode modification, 5  $\mu\text{L}$  of suspensions were drop-cast onto bare GC electrodes and dried under a lamp. Inherent electrochemistry was studied by CV in nitrogen-purged conditions at a scan rate of  $100 \text{ mV s}^{-1}$  in  $50 \times 10^{-3} \text{ M}$ , pH 7.0 PBS. Electrochemical sensing of  $1.0 \times 10^{-3} \text{ M}$  ascorbic acid,  $0.1 \times 10^{-3} \text{ M}$  uric acid, and  $0.1 \times 10^{-3} \text{ M}$  dopamine was similarly conducted by CV at a scan rate of  $100 \text{ mV s}^{-1}$  in  $50 \times 10^{-3} \text{ M}$ , pH 7.0 PBS. HET studies were conducted by CV with  $10 \times 10^{-3} \text{ M}$  ferro/ferricyanide  $[\text{Fe}(\text{CN})_6]^{4-/3-}$  redox probe at a scan rate of  $100 \text{ mV s}^{-1}$  in potassium chloride (0.1 M) as supporting electrolyte. The  $k_{\text{obs}}^0$  values were calculated by Nicholson's method<sup>[79]</sup> that correlated to the obtained  $\Delta E_p$  values. Electrocatalytic performance toward HER was investigated by linear sweep voltammetry (scan rate of  $2 \text{ mV s}^{-1}$  in  $0.5 \text{ M H}_2\text{SO}_4$ ) with bare GC as counter electrode. Electrocatalytic performance toward ORR was studied by linear sweep voltammetry in both purged and ambient conditions (scan rate of  $5 \text{ mV s}^{-1}$  with  $0.1 \text{ M KOH}$ ). All measurements were conducted relative to Ag/AgCl reference electrode and Pt counter electrode unless otherwise stated.

**Cytotoxicity Assessments:** Materials were dispersed in ultrapure water ( $500 \mu\text{g mL}^{-1}$ ) and subjected to 1 h of ultrasonication. Culturing of A549 (Bio-Rev, Singapore), MCF-7, HepG2, and HEK-293 cells (ATCC, Manassas, VA, USA) were at  $37$  °C with 5%  $\text{CO}_2$  in cell culture media (CCM). CCM consists of Dulbecco's Modified Eagle medium (DMEM), 10% fetal bovine serum (FBS) (Life Technologies, Singapore), and 1% penicillin/streptomycin (Capricorn). Cells were seeded (3000 cells per well) in a 96-well plate and cultured for 24 h. After 24 h, CCM was removed and replaced with varying concentrations of material suspensions prepared in fresh CCM ( $100 \mu\text{L}$  per well) and further incubated for 24 h. Negative control was cells that were only exposed to CCM and background were materials in CCM in the absence of cells. Subsequently,  $10 \mu\text{L}$  per well of WST-8 reagent (Dojindo, Japan) was added and incubated for another hour for the quantification of cell viabilities. After 1 h, absorbance was measured at 450 nm and absorbance spectrum from 350 to 550 nm was obtained.

### Supporting Information

Supporting Information is available from the Wiley Online Library or from the author.

### Acknowledgements

M.P. acknowledges the financial support of Grant Agency of the Czech Republic (EXPRO: 19–26896X). J.S. acknowledges the financial support of Grant Agency of the Czech Republic (GACR: 19–17593Y). This research was supported by the National Research Foundation, Prime Minister's Office, Singapore under its CREATE program.

### Conflict of Interest

The authors declare no conflict of interest.

## Keywords

energy, layered materials, nanomaterials, sensing, toxicity

Received: December 6, 2019

Revised: February 28, 2020

Published online:

- [1] K. S. Novoselov, A. K. Geim, S. V. Morozov, D. Jiang, Y. Zhang, S. V. Dubonos, I. V. Grigorieva, A. A. Firsov, *Science* **2004**, 306, 666.
- [2] P. Vishnoi, K. Pramoda, C. N. R. Rao, *ChemNanoMat* **2019**, 5, 1062.
- [3] S. Balendhran, S. Walia, H. Nili, S. Sriram, M. Bhaskaran, *Small* **2015**, 11, 640.
- [4] X. Kong, Q. Liu, C. Zhang, Z. Peng, Q. Chen, *Chem. Soc. Rev.* **2017**, 46, 2127.
- [5] I. Gablech, J. Pekárek, J. Klempa, V. Svatoš, A. Sajedi-Moghaddam, P. Neužil, M. Pumera, *TrAC, Trends Anal. Chem.* **2018**, 105, 251.
- [6] T. Hartman, Z. Sofer, *ACS Nano* **2019**, 13, 8566.
- [7] C. N. R. Rao, K. Pramoda, *Bull. Chem. Soc. Jpn.* **2019**, 92, 441.
- [8] M. Long, P. Wang, H. Fang, W. Hu, *Adv. Funct. Mater.* **2019**, 29, 1803807.
- [9] R. K. Ulaganathan, Y.-H. Chang, D.-Y. Wang, S.-S. Li, *Bull. Chem. Soc. Jpn.* **2018**, 91, 761.
- [10] S. Cahangirov, M. Topsakal, E. Aktürk, H. Sahin, S. Ciraci, *Phys. Rev. Lett.* **2009**, 102, 236804.
- [11] K. Takeda, K. Shiraishi, *Phys. Rev. B* **1994**, 50, 14916.
- [12] A. Molle, J. Goldberger, M. Houssa, Y. Xu, S.-C. Zhang, D. Akinwande, *Nat. Mater.* **2017**, 16, 163.
- [13] Z. Ni, Q. Liu, K. Tang, J. Zheng, J. Zhou, R. Qin, Z. Gao, D. Yu, J. Lu, *Nano Lett.* **2012**, 12, 113.
- [14] J. Zhu, A. Chronos, U. Schwingenschlögl, *Nanoscale* **2016**, 8, 7272.
- [15] F. Wohler, *Ann. Chem. Pharm.* **1863**, 127, 257.
- [16] A. Weiss, G. Beil, H. Meyer, *Z. Naturforsch. B* **1980**, 35, 25.
- [17] J. R. Dahn, B. M. Way, E. Fuller, *Phys. Rev. B* **1993**, 48, 17872.
- [18] H. Nakano, M. Ishii, H. Nakamura, *Chem. Commun.* **2005**, 23, 2945.
- [19] S. Li, H. Wang, D. Li, X. Zhang, Y. Wang, J. Xie, J. Wang, Y. Tian, W. Nic, Y. Xie, *J. Mater. Chem. A* **2016**, 4, 15841.
- [20] G. Vogg, M. S. Brandt, M. Stutzmann, *Adv. Mater.* **2000**, 12, 1278.
- [21] A. Nijamudheen, R. Bhattacharjee, S. Choudhury, A. Datta, *J. Phys. Chem. C* **2015**, 119, 3802.
- [22] E. Bianco, S. Butler, S. Jiang, O. D. Restrepo, W. Windl, J. E. Goldberger, *ACS Nano* **2013**, 7, 4414.
- [23] S. Jiang, S. Butler, E. Bianco, O. D. Restrepo, W. Windl, J. E. Goldberger, *Nat. Commun.* **2014**, 5, 3389.
- [24] Y. Jing, X. Zhang, D. Wu, X. Zhao, Z. Zhou, *J. Phys. Chem. Lett.* **2015**, 6, 4252.
- [25] L. C. Loaiza, L. Monconduit, V. Seznec, *J. Power Sources* **2019**, 417, 99.
- [26] K. Krishnamoorthy, P. Pazhamalai, S.-J. Kim, *Energy Environ. Sci.* **2018**, 11, 1595.
- [27] Z. Liu, Z. Lou, Z. Li, G. Wang, Z. Wang, Y. Liu, B. Huang, S. Xia, X. Qin, X. Zhang, Y. Dai, *Chem. Commun.* **2014**, 50, 11046.
- [28] Z. Liua, Y. Daia, Z. Zheng, B. Huang, *Catal. Commun.* **2019**, 118, 46.
- [29] T. Maric, S. M. Beladi-Mousavi, B. Khezri, J. Sturala, M. Z. M. Nasir, R. D. Webster, Z. Sofer, M. Pumera, *Small* **2019**, 1902365.
- [30] Z. Liu, Z. Wang, Q. Sun, Y. Dai, B. Huang, *Appl. Surf. Sci.* **2019**, 467–468, 881.
- [31] P. Pazhamalai, K. Krishnamoorthy, S. Sahoo, V. K. Mariappan, S.-J. Kim, *ACS Appl. Mater. Interfaces* **2019**, 11, 624.
- [32] S. J. Kerber, J. J. Bruckner, K. Wozniak, S. Seal, S. Hardcastle, T. L. Barr, *J. Vac. Sci. Technol., A* **1996**, 14, 1314.
- [33] J. Vilcarrmero, F. C. Marques, J. Andreu, *J. Non-Cryst. Solids* **1998**, 227–230, 427.
- [34] J. Vilcarrmero, F. C. Marques, *Appl. Phys. A: Mater. Sci. Process.* **2000**, 70, 581.
- [35] U. Dettlaff-Weglikowska, W. Hönlle, A. Molassioti-Dohms, S. Finkbeiner, J. Weber, *Phys. Rev. B* **1997**, 56, 13132.
- [36] S. Jiang, K. Krymowski, T. Asel, M. Q. Arguilla, N. D. Cultrara, E. Yanchenko, X. Yang, L. J. Brillson, W. Windl, J. E. Goldberger, *Chem. Mater.* **2016**, 28, 8071.
- [37] J. Sturala, J. Luxa, S. Matějková, Z. Sofer, M. Pumera, *Nanoscale* **2019**, 11, 19327.
- [38] S. Jiang, M. Q. Arguilla, N. D. Cultrara, J. E. Goldberger, *Chem. Mater.* **2016**, 28, 4735.
- [39] M. Z. M. Nasir, Z. Sofer, A. Ambrosi, M. Pumera, *Nanoscale* **2015**, 7, 3126.
- [40] H. S. Toh, A. Ambrosi, C. K. Chua, M. Pumera, *J. Phys. Chem. C* **2011**, 115, 17647.
- [41] Z. Meng, R. M. Stolz, L. Mendecki, K. A. Mirica, *Chem. Rev.* **2019**, 119, 478.
- [42] M. Z. M. Nasir, M. Pumera, *TrAC, Trends Anal. Chem.* **2019**, 121, 115696.
- [43] H. Zhang, *ACS Nano* **2015**, 9, 9451.
- [44] J. M. Beaulieu, R. R. Gainetdinov, *Pharmacol. Rev.* **2011**, 63, 182.
- [45] K. Jackowska, P. Kryszinski, *Anal. Bioanal. Chem.* **2013**, 405, 3753.
- [46] M. Sajid, M. K. Nazal, M. Mansha, A. Alsharaa, S. M. S. Jillani, C. Basheer, *TrAC, Trends Anal. Chem.* **2016**, 76, 15.
- [47] C.-L. Sun, C.-T. Chang, H.-H. Lee, J. Zhou, J. Wang, T.-K. Sham, W.-F. Pong, *ACS Nano* **2011**, 5, 7788.
- [48] R. A. Hearle, N. M. Latiff, Z. Sofer, V. Mazánek, M. Pumera, *Electroanalysis* **2017**, 29, 45.
- [49] S. R. Ali, Y. Ma, R. R. Parajuli, Y. Balogun, W. Y.-C. Lai, H. He, *Anal. Chem.* **2007**, 79, 2583.
- [50] Y. Wang, Y. Li, L. Tang, J. Lu, J. Li, *Electrochem. Commun.* **2009**, 11, 889.
- [51] B. R. Liyarita, A. Ambrosi, M. Pumera, *Electroanalysis* **2018**, 30, 1319.
- [52] U. E. Majewska, K. Chmurski, K. Biesiada, A. R. Olszyna, R. Bilewicz, *Electroanalysis* **2006**, 18, 1463.
- [53] R. Ramachandran, X. Leng, C. Zhao, Z.-X. Xu, F. Wang, *Appl. Mater. Today* **2020**, 18, 100477.
- [54] M. Shao, Q. Chang, J.-P. Dodelet, R. Chenitz, *Chem. Rev.* **2016**, 116, 3594.
- [55] B. E. Conway, B. V. Tilak, *Electrochim. Acta* **2002**, 47, 3571.
- [56] J. K. Nørskov, T. Bligaard, A. Logadottir, J. R. Kitchin, J. G. Chen, S. Pandalov, U. Stimming, *J. Electrochem. Soc.* **2005**, 152, J23.
- [57] Y. Zheng, Y. Jiao, M. Jaroniec, Y. Jin, S. Z. Qiao, *Small* **2012**, 8, 3550.
- [58] D. Voiry, M. Chhowalla, Y. Gogotsi, N. A. Kotov, Y. Li, R. M. Penner, R. E. Schaak, P. S. Weiss, *ACS Nano* **2018**, 12, 9635.
- [59] C. G. Morales-Guio, L.-A. Stern, X. Hu, *Chem. Soc. Rev.* **2014**, 43, 6555.
- [60] J. G. N. Thomas, *Trans. Faraday Soc.* **1961**, 57, 1603.
- [61] R. Gusmão, Z. Sofer, D. Bousa, M. Pumera, *Angew. Chem.* **2017**, 129, 14609.
- [62] L. Wang, Z. Sofer, A. Ambrosi, P. Štěrba, M. Pumera, *Electrochem. Commun.* **2014**, 46, 148.
- [63] J. Benson, Q. Xu, P. Wang, Y. Shen, L. Sun, T. Wang, M. Li, P. Papakonstantinou, *ACS Appl. Mater. Interfaces* **2014**, 6, 19726.
- [64] L. Wang, A. Ambrosi, M. Pumera, *Angew. Chem., Int. Ed.* **2013**, 52, 13818.
- [65] A. Y. S. Eng, A. Ambrosi, Z. Sofer, P. Simek, M. Pumera, *ACS Nano* **2014**, 8, 12185.
- [66] R. J. Toh, Z. Sofer, M. Pumera, *J. Mater. Chem. A* **2016**, 4, 18322.
- [67] X. Chia, A. Ambrosi, P. Lazar, Z. Sofer, M. Pumera, *J. Mater. Chem. A* **2016**, 4, 14241.
- [68] R. J. Toh, Z. Sofer, M. Pumera, *ChemPhysChem* **2015**, 16, 3527.

- [69] D. van der Merwe, J. A. Pickrell, in *Veterinary Toxicology*, 3rd ed. (Ed: R. C. Gupta), Academic Press, London **2018**, p. 319.
- [70] S. C. Sahu, A. W. Hayes, *Toxicol. Res. Appl.* **2017**, *1*, 239784731772635.
- [71] M. Ishiyama, Y. Miyazono, M. Shiga, K. Sasamoto, Water-Soluble Tetrazolium Salt Compounds, *U.S. Patent 6063587A*, **2000**.
- [72] Q. Wang, Y. Bao, X. Zhang, P. R. Coxon, U. A. Jayasooriya, Y. Chao, *Adv. Healthcare Mater.* **2012**, *1*, 189.
- [73] J.-W. Yun, S.-H. Kim, J.-R. You, W. H. Kim, J.-J. Jang, S.-K. Min, H. C. Kim, D. H. Chung, J. Jeong, B.-C. Kang, J.-H. Che, *J. Appl. Toxicol.* **2015**, *35*, 681.
- [74] J.-H. Park, L. Gu, G. v. Maltzahn, E. Ruoslahti, S. N. Bhatia, M. J. Sailor, *Nat. Mater.* **2009**, *8*, 331.
- [75] Y.-H. Ma, C.-P. Huang, J.-S. Tsai, M.-Y. Shen, Y. K. Li, L.-Y. Lin, *Toxicol. Lett.* **2011**, *207*, 258.
- [76] N. M. Latiff, W. Z. Teo, Z. Sofer, S. Huber, A. C. Fisher, M. Pumera, *RSC Adv.* **2015**, *5*, 67485.
- [77] N. M. Latiff, W. Z. Teo, Z. Sofer, A. C. Fisher, M. Pumera, *Chem. - Eur. J.* **2015**, *21*, 13991.
- [78] S. Yamanaka, H. Matsu-ura, M. Ishikawa, *Mater. Res. Bull.* **1996**, *31*, 307.
- [79] R. S. Nicholson, *Anal. Chem.* **1965**, *37*, 1351.